

## ADDITIONAL *SPITZER* IRS SPECTROSCOPY OF THREE INTERMEDIATE POLARS: THE DETECTION OF A MID-INFRARED SYNCHROTRON FLARE FROM V1223 SAGITTARI<sup>\*</sup>

THOMAS E. HARRISON<sup>1</sup>, JILLIAN BORNAK<sup>1</sup>, MICHAEL P. RUPEN<sup>2</sup>, AND STEVE B. HOWELL<sup>3</sup>

<sup>1</sup> Department of Astronomy, New Mexico State University, P.O. Box 30001, MSC 4500, Las Cruces, NM 88003-8001, USA; [tharriso@nmsu.edu](mailto:tharriso@nmsu.edu), [jbornak@nmsu.edu](mailto:jbornak@nmsu.edu)

<sup>2</sup> National Radio Astronomy Observatory, 1003 Lopezville Road, Socorro, NM 87801, USA; [mrupen@aoc.nrao.edu](mailto:mrupen@aoc.nrao.edu)

<sup>3</sup> WIYN Observatory and National Optical Astronomy Observatories, 950 North Cherry Avenue, Tucson, AZ 85726, USA; [howell@noao.edu](mailto:howell@noao.edu)

Received 2009 September 9; accepted 2009 December 15; published 2010 January 18

### ABSTRACT

We present new *Spitzer* Infrared Spectrograph (IRS) observations of three intermediate polars: V1223 Sgr, EX Hya, and V603 Aql. We detected a strong, fading flare event from V1223 Sgr. During this event, the flux declined by a factor of 13 in 30 minutes. Given the similarity in the slope of its mid-infrared spectrum during this event to that of AE Aqr, we suggest that this event was caused by transient synchrotron emission. Thus, V1223 Sgr becomes the third cataclysmic variable known to be a synchrotron source. We were unable to confirm the mid-infrared excess noted by Harrison et al. (Paper I) for EX Hya, suggesting that this object is either not a synchrotron source, or is slightly variable. Due to a very high background, V603 Aql was not detected in the long-wavelength regions accessible to the IRS. Given the recent detection of SS Cygni at radio wavelengths during outburst, we extract archival *Spitzer* IRS spectra for this source obtained during two successive maxima. These spectra do not show a strong excess, but without simultaneous data at shorter wavelengths, it is not possible to determine whether there is any contribution to the mid-infrared fluxes from a synchrotron jet.

**Key words:** infrared: stars – stars: individual (V603 Aquilae, SS Cygni, PQ Geminorum, EX Hydrae, V1223 Sagittarii)

### 1. INTRODUCTION

Intermediate polars (IPs) are a heterogeneous subclass of cataclysmic variable (CV) with magnetic white dwarf primaries that are accreting matter from low mass, late-type secondary stars. They can be differentiated from the highly magnetic “polars” in that they exhibit X-ray periodicities that are substantially shorter than their orbital periods. These periods are believed to be due to the accretion region(s) rotating into the line of sight. Thus, unlike polars, their white dwarfs are rotating asynchronously (see Ramsay et al. 2008, and references therein). In addition, the X-ray spectra of IPs tend to be harder than those of polars. It is believed that the magnetic field strength of the white dwarf in IPs is lower than in polars based on the lack of strong polarization or discrete cyclotron harmonics in their optical/near-infrared spectra (Wickramasinghe et al. 1991). In the typical polar, the accretion stream is captured close to the secondary star, and funneled directly onto the white dwarf. In the majority of IPs, a truncated accretion disk appears to be present, and the capture of the inner portion of this stream at the magnetospheric radius creates accretion “curtains” that absorb some of the soft X-ray flux, hardening their spectra (see Hellier et al. 1996, and references therein).

Harrison et al. (2007, hereafter “Paper I”) used mid-infrared spectra obtained by the Infrared Spectrograph (IRS) on *Spitzer* to search for cyclotron emission from 11 IPs. If the magnetic field strength of the white dwarfs in IPs was  $B \geq 1$  MG, cyclotron harmonic emission (even if optically thick) would appear in the

5–21  $\mu\text{m}$  bandpass. No evidence for cyclotron emission from these 11 systems was found, with the result being that their mid-IR spectra were simple power-law extrapolations of their optical/near-IR spectral energy distributions (SEDs). In that study, however, three systems proved to be interesting: AE Aqr, EX Hya, and V1223 Sgr. AE Aqr exhibited a dramatic upturn in its spectrum beyond 14  $\mu\text{m}$ , which was clearly the detection of optically thin synchrotron emission from this system. Both EX Hya and V1223 Sgr showed a flattening of their spectra at the red ends of their IRS spectra, suggesting that they might also be synchrotron sources.

If either EX Hya or V1223 Sgr were synchrotron sources like AE Aqr, then their spectra should exhibit a dramatic upturn in flux at the longest wavelengths ( $\sim 38$   $\mu\text{m}$ ) accessible with the IRS. Thus, we initiated a new study to obtain deeper IRS spectra in the long-wavelength bandpasses of the IRS for both systems. In addition, we obtained identical observations for V603 Aql, the optically brightest IP.

AE Aqr has long been known as the only CV that had detectable synchrotron emission. It has been expected by some (e.g., Livio 1999; Soker & Lasota 2004) that CVs should be synchrotron sources, and the identification of such emission would show that all accreting binaries with compact primaries emit such radiation. With the recent detection of a synchrotron jet from SS Cygni during outburst (Körding et al. 2008), one of the previously unique features of AE Aqr has been matched. The question still remains as to the universality of synchrotron emission from CVs. As shown by the results for low mass X-ray binaries (Migliari & Fender 2006; Gallo et al. 2007; Gelino et al. 2010), the mid-infrared is an ideal bandpass in which to search for optically thin synchrotron emission.

In addition to the new observations of EX Hya, V1223 Sgr, and V603 Aql, we present archival *Spitzer* observations of SS Cygni that show a weak mid-IR excess that we discuss in the context of the synchrotron jet detected for this system. We describe these observations in the following section, where we

<sup>\*</sup> Includes observations obtained at the Gemini Observatory, which is operated by the Association of Universities for Research in Astronomy, Inc., under a cooperative agreement with the NSF on behalf of the Gemini partnership: the National Science Foundation (United States), the Science and Technology Facilities Council (United Kingdom), the National Research Council (Canada), CONICYT (Chile), the Australian Research Council (Australia), Ministério da Ciência e Tecnologia (Brazil), and Ministerio de Ciencia, Tecnología e Innovación Productiva (Argentina).

**Table 1**  
*Spitzer* Observation Journal and Program Object Characteristics

Object	Obs. Date	U.T. Start	LL2 (No. × Exp. Time)	LL1 (No. × Exp. Time)	$P_{\text{orb}}$ (hr)	$P_{\text{spin}}$ (minutes)
V603 Aql	2008 Nov 13	04:49:54	30 × 121.9 s	30 × 121.9 s	3.32	61
EX Hya	2009 Feb 21	18:18:27	30 × 121.9 s	30 × 121.9 s	1.64	67
V1223 Sgr	2008 Nov 6	21:57:49	30 × 121.9 s	30 × 121.9 s	3.37	61

present new near-infrared spectra of V1223 Sgr, EX Hya, and PQ Gem, present the results for the *Spitzer* observations in Section 3, discuss these results in Section 4, and present our conclusions in Section 5.

## 2. OBSERVATIONS

### 2.1. *Spitzer* Observations

The IRS on the *Spitzer Space Telescope* has been described by Houck et al. (2004). The IRS provides spectra from 5.2 to 38  $\mu\text{m}$  at resolutions of  $R \sim 90$  and 600. The data for the IPs presented below were all obtained in the low-resolution mode. Because the signal-to-noise ratio (S/N) of the IRS spectra for V603 Aql, EX Hya, and V1223 Sgr were all rather low in our first effort (we did not even detect V603 Aql beyond 14  $\mu\text{m}$ ), we increased the total, on-source exposure times from 1200 s used in the first epoch LL2 (14–21  $\mu\text{m}$ ) bandpass observations, to 3657 s used here. In addition, we obtained new observations in the LL1 (19.5–38  $\mu\text{m}$ ) bandpass, duplicating the LL2 exposure times for the three IPs. For each object, observations at two slit positions were obtained so as to allow for proper sky subtraction. The observation log can be found in Table 1.

We extracted all of the spectra using the SPICE package after constructing median sky images that were subsequently subtracted off of the individual spectra. In the case of V1223 Sgr, for which we extract temporally resolved spectra, we performed the additional process of applying a “rogue pixel mask” (using `b2_rmask_IRS56`) to the data using the IDL software routine “IRSCLEAN”.<sup>4</sup> This step helps eliminate spurious pixels in the data that can impart emission or absorption features to low S/N spectra.

As described later, we detected both EX Hya and V1223 Sgr in both the LL1 and LL2 spectra, including an apparent transient event in the LL2 data of the latter object. We did not, however, detect V603 Aql even though it is visually brighter than either EX Hya or V1223 Sgr. The mid-IR background in the region around V603 Aql is very high, and thus we were unable to investigate its spectrum to the same low flux levels as the other two sources.

### 2.2. Near-infrared Spectra

In Paper I, we presented near-IR spectra for five of the 11 IPs surveyed there. In order to present a fuller picture of this class of objects, we present similar spectra of three of the IPs in that paper for which we did not have data at that time: EX Hya, V1223 Sgr, and PQ Gem. These data were obtained using GNIRS<sup>5</sup> on Gemini-south. GNIRS produces cross-dispersed spectra covering the *J*, *H*, and *K* bands, and we used the 0.3 slit and the 32 l mm<sup>-1</sup> grating to produce a dispersion of  $R \approx 3400$

**Table 2**  
GNIRS Observation Journal

Object	Obs. Date	U.T. Start	No. of Exposures	Exp. Time (s)
V1223 Sgr	2007 Mar 29	07:52:52	24	122
PQ Gem	2007 Mar 30	00:12:04	30	122
EX Hya	2007 Mar 30	02:08:03	50	120

in the *K* band. These observations were obtained under the “poor weather” proposal GS-2007A-Q-70. The seeing was quite poor (FWHM = 1.8) during these observations, but the skies appeared to be photometric, as the fluxes of the individual spectra did not vary dramatically between exposures. A log of these observations is presented in Table 2. These data were reduced using IRAF, and tellurically corrected using AOV stars that were observed shortly before, or after, the program object. After division by the AOV star, the spectra were multiplied by a model atmosphere spectrum of Vega in order to reduce the impact of the H I absorption lines present in the telluric standard star spectra.

These spectra are presented in Figure 1 and cover the range from 8200 Å to 2.5  $\mu\text{m}$  in five spectral orders. The plotted spectra have been truncated in regions (near the ends of the various orders) where the S/N was very poor. Rough estimates of the *K*-band magnitudes indicate that both PQ Gem ( $K \sim 12.3$ ), and V1223 Sgr ( $K \sim 12.3$ ) were at similar brightness levels to the values listed in the Two Micron All Sky Survey (2MASS) catalog. EX Hya, however, was 2 mag brighter ( $K \sim 9.5$ ) than its 2MASS value. The AAVSO database indicates that EX Hya was at the visual maximum of an outburst at the time of the GNIRS observations. Like the results presented in Paper I, these spectra show no evidence for cyclotron emission in the covered wavelength interval. All of the prominent emission lines are due to H I and He I. All three objects have an emission line at 1.163  $\mu\text{m}$  that we attribute to He II. EX Hya also shows evidence for He II emission at 2.19  $\mu\text{m}$ , but this line is blended with the broad H I Br  $\gamma$  emission line. All three objects have a weak emission line at 1.1755  $\mu\text{m}$  that does not appear to be due to either hydrogen or helium. As noted in Paper I, in quiescence, the secondary star in EX Hya is visible in the near-IR. As shown in Figure 1(a), even in the middle of an outburst, there is evidence for absorption from the water vapor features at 1.38 and 1.90  $\mu\text{m}$ , as well as the Na I doublet at 2.2  $\mu\text{m}$ .

## 3. RESULTS

For this second epoch of *Spitzer* observations, we obtained double the exposure time of the original LL2 observations, and an identical amount of observation time in the LL1 bandpass in a hope to provide a higher S/N detection of the long-wavelength spectra of the three IPs. Unfortunately, as noted above, we did not detect V603 Aql in either bandpass due to a very high mid-infrared background. The galactic latitude of V603 Aql is only  $b = +0.8$ , and the *IRAS* maps show significant 25 and 60  $\mu\text{m}$

<sup>4</sup> [http://ssc.spitzer.caltech.edu/archanaly/contributed/irsclean/IRSCLEAN\\_MASK.html](http://ssc.spitzer.caltech.edu/archanaly/contributed/irsclean/IRSCLEAN_MASK.html)

<sup>5</sup> <http://www.gemini.edu/sciops/instruments/gnirs>

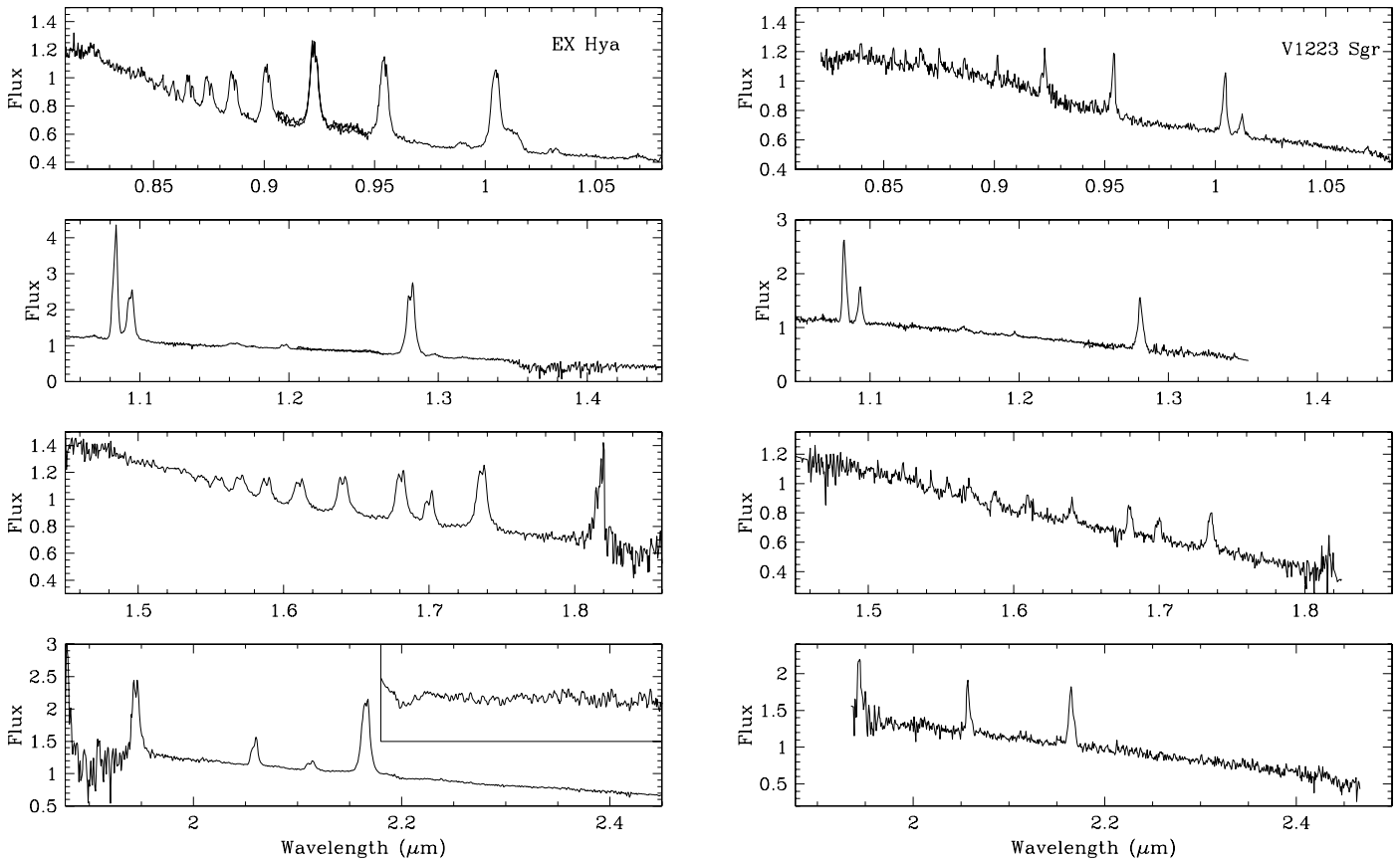


**Figure 1.** GNIRS spectra of EX Hya, V1223 Sgr, and PQ Gem. The spectra in the individual orders have been normalized for presentation purposes. In addition, we have added an inset into the *K*-band panel for EX Hya to show that the Na I doublet at 2.20  $\mu\text{m}$  is clearly visible.

emission at this location. We did detect both EX Hya and V1223 Sgr in both bands, and present those results here.

### 3.1. EX Hya

As noted in Paper I, EX Hya has the longest white dwarf spin period ( $P_{\text{spin}} = 67$  minutes) of any of our program objects. In fact, the ratio of its spin period to the orbital period,  $P_{\text{spin}}/P_{\text{orb}} = 0.68$ , is the largest of all of the conventional IPs (see the tabulation by Norton et al. 2004). EX Hya also has a large orbital inclination angle,  $i = 77^\circ$  (Ritter & Kolb 2003), and this is evident from the double peaked emission lines seen in the near-IR spectrum shown in Figure 1(a). But the emission line profiles change dramatically over an orbit. Our GNIRS data spanned 1.5 orbital periods of EX Hya, and we show the evolution of the spectra in the *K* band over this time period in Figure 2. Belle et al. (2005) present the evolution of the line profiles of the optical H I lines over a full orbit of EX Hya, and the behavior of those lines was remarkably similar to that of the infrared line profiles.

In Paper I, we found a weak excess in the LL2 data for EX Hya. We reproduce the observed SED of EX Hya in Figure 3. The black, filled circles in this diagram are the data from Paper I. While the LL2 spectrum in the first epoch data was clearly visible, the fluxes of the individual resolution elements in the extracted spectrum had  $S/N \sim 1$ . Thus, the spectrum was rebinned into 1  $\mu\text{m}$  wavelength intervals to produce the data points in Figure 3. Superficially, the second epoch spectra looked to have a similar  $S/N$ , even though the exposure time

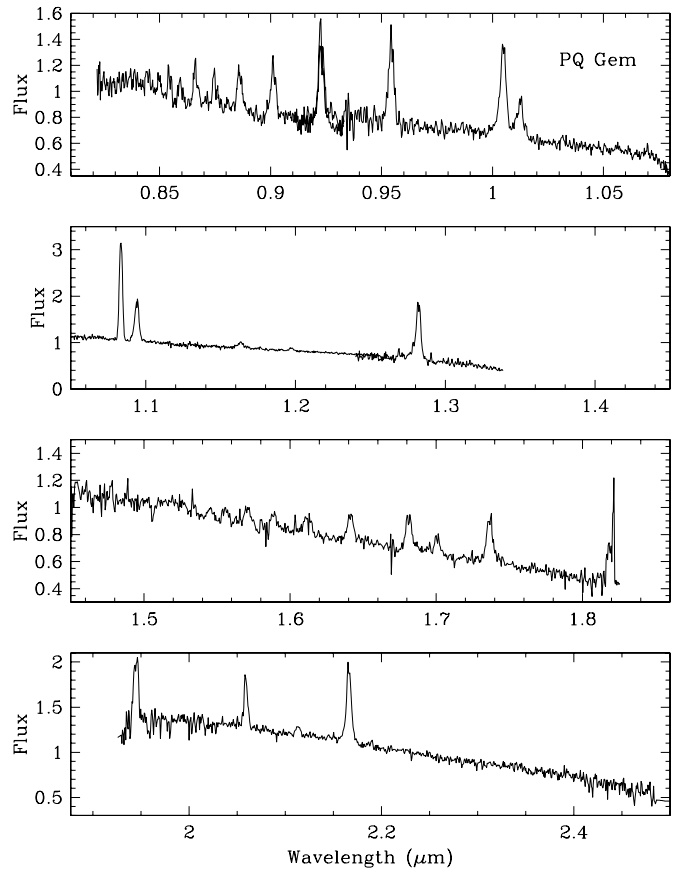


**Figure 1.** (Continued)

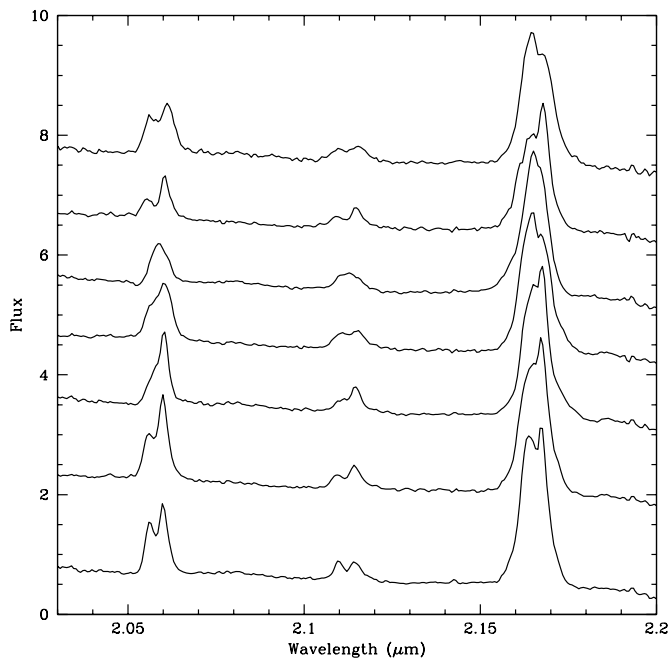


**Figure 2.** Changing line profiles seen in EX Hya over an orbital period. The seven plotted spectra were obtained at 14 minute intervals. The strongest emission lines are due to He I at 2.06 and 2.11  $\mu\text{m}$ , and H I Br $\gamma$  at 2.16  $\mu\text{m}$ .

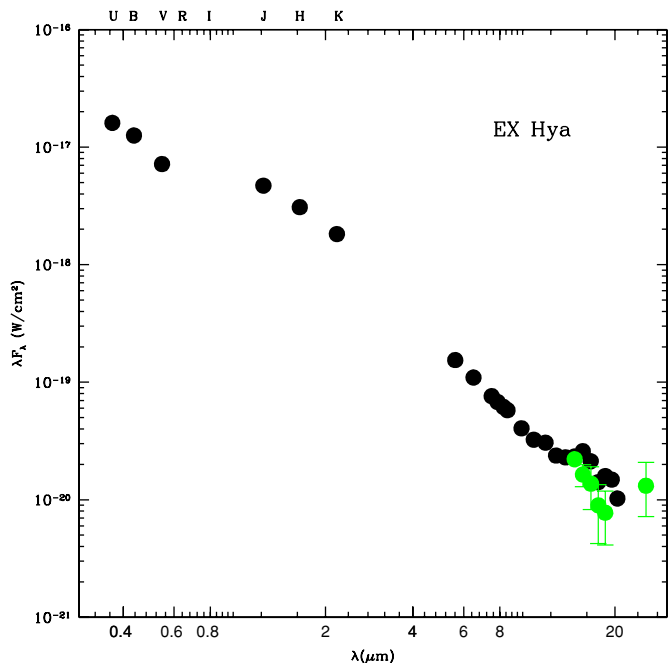


**Figure 3.** SED of EX Hya. The black points are from Paper I, while the green symbols are from the new observations. See Paper I for the error bars on the first epoch data set.

was twice that of the original data. The result, shown in green, is that the second epoch LL2 spectrum appears to show no excess, and is consistent with the extrapolation of the SED from the 0.4 to 20  $\mu\text{m}$ .

In the longer wavelength LL1 data set, EX Hya was barely detectable, only being visible in the co-added, background-subtracted data from  $\sim 20.5$  to 30.5  $\mu\text{m}$ . We thus averaged the final extracted LL1 spectrum over this range to produce a single datum at  $\langle \lambda \rangle = 25.5$   $\mu\text{m}$ . While this point seems to indicate an excess, it has significant error bars ( $S/N \sim 2$ ), and it is therefore

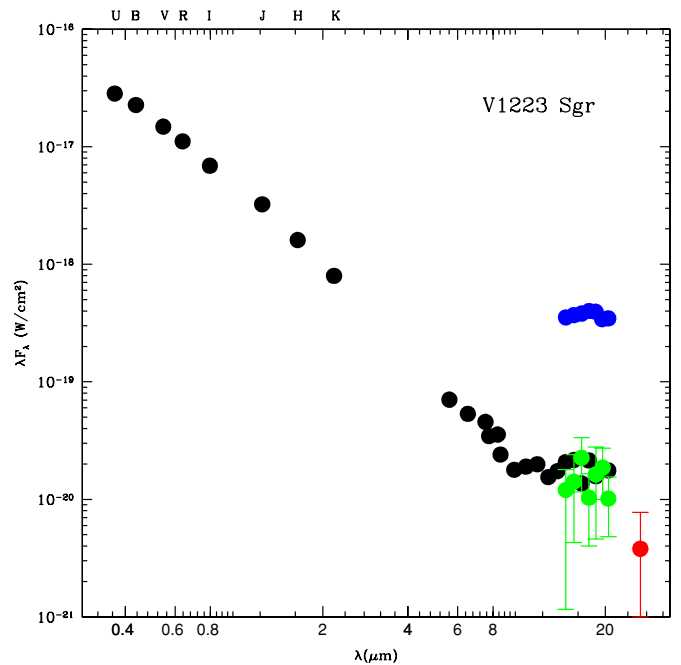


**Figure 4.** SED of V1223 Sgr. As in Figure 3, the black circles are from Paper I. The blue circles are the mean of the first three LL2 spectra rebinned into 1  $\mu\text{m}$  intervals, while the green circles are the mean of the last three spectra in the LL2 sequence with the same binning. The red datum is the mean flux from the LL1 data set. Error bars are shown when larger than the symbol size (see Paper I for the errors on the first epoch LL2 spectrum).

consistent with the overall SED. We conclude that, given the low  $S/N$  for both epochs of data, there is no significant evidence for a mid-infrared excess from EX Hya.

### 3.2. V1223 Sgr

The GNIRS spectra of V1223 Sgr show sharper emission line profiles than seen in EX Hya, indicative of its almost face-on inclination angle of  $i = 13^\circ$  (Ritter & Kolb 2003). Note that the He I emission lines in the spectra of V1223 Sgr are stronger, relative to H I, than those seen in EX Hya. As might be expected, there was no significant evolution of the line profiles over the 45 minutes covered by the GNIRS data set. There is also no evidence for the presence of a secondary star in these data.

In our first epoch of *Spitzer* observations, the LL2 spectrum of V1223 Sgr had a similar flux level to that observed for EX Hya<sup>6</sup>. Thus, it was surprising when the first spectrum in the LL2 sequence for V1223 Sgr showed a very bright source. In Figure 4, we present the first epoch SED for V1223 Sgr, with the new data overplotted. The blue points in this plot are the average fluxes of the first three spectra in the LL2 sequence. The green data points are the average of the last three spectra in the LL2 sequence. The last three spectra were obtained about 30 minutes after first spectrum in the LL2 sequence. In the 0.6 hr of the LL2 spectral sequence, the mean flux declined from a peak value of  $0.026 \pm 0.003$  Jy to  $0.002 \pm 0.002$  Jy.

We show the spectral evolution of the LL2 observations in Figure 5. The fluxes of the first two spectra in the sequence are similar, but after that, the decline is monotonic until “quiescence.” While the individual spectra are quite noisy, it is clear that the spectra maintain the same shape throughout the decline. The light curve is presented in Figure 6. Unfortunately,

<sup>6</sup> Note that the unit on the y-axis of all the spectra presented in Figure 2 of Paper I should have been denoted as Jy, not mJy.



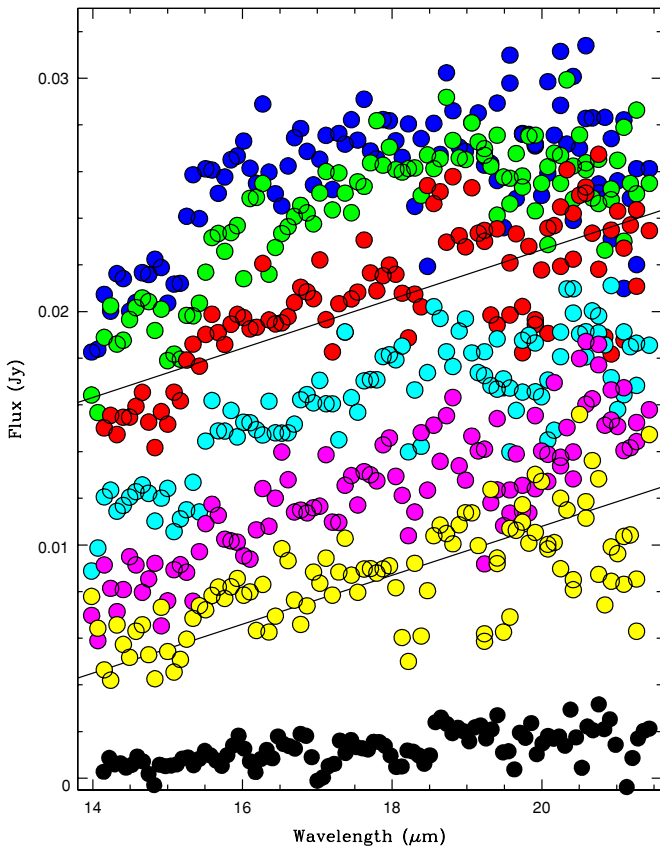


**Figure 5.** Temporal evolution of the first six LL2 spectra, and the mean of the final three spectra. The spectra were obtained at 2.5 minute intervals. A least-squares fit to the third spectrum (red) is plotted, and then scaled to the sixth spectrum to demonstrate that the spectra maintained the same shape throughout the initial decline.

we did not capture the entire event, so we do not know the peak flux, but the similar fluxes of the first two spectra in the sequence may indicate that these observations were close to the peak flux of this event and, if true, suggests that it did not greatly exceed 0.03 Jy.

By the time of the LL1 observations, V1223 Sgr had faded to the point where it was almost undetectable. Like the data set for EX Hya, we have produced an average flux for the LL1 data, and this flux is consistent with a simple extension of the optical/near-IR SED.

#### 4. DISCUSSION

The inference from the first epoch *Spitzer* observations of EX Hya and V1223 Sgr was that they had mid-infrared excesses beyond 14  $\mu\text{m}$ , similar in shape to that observed for the much brighter IP AE Aqr. Our second epoch observations do not confirm the excess for EX Hya, suggesting that this object is either slightly variable, or that the excess derived from the first epoch observations was in error due to flux calibration issues that could arise for such a faint source. Due to a very high mid-infrared background, we were unable to detect V603 Aql. The second epoch observations of V1223 Sgr were far more interesting, in that we were fortunate enough to detect the decline from a “flare” from this source.

What was the nature of this event? If we take the average of the last few LL2 spectra and call that quiescence, then V1223 Sgr brightened by at least a factor of 13. As noted in Harrison et al. (2004), a visual flare of  $\Delta v = 1.2$  mag was

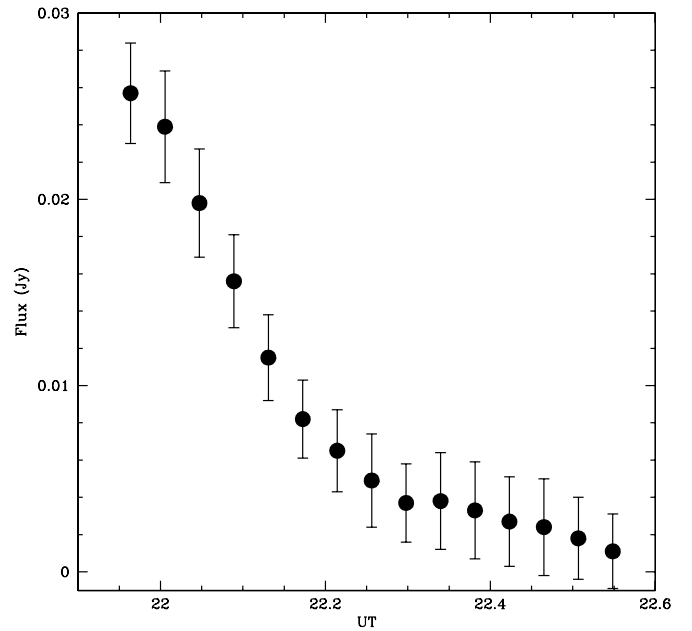


**Figure 6.** Light curve of V1223 Sgr using the mean LL2 flux from each individual spectrum.

observed by van Amerongen & van Paradijs (1989), but this appears to be the only “outburst” of this amplitude ever seen for this object. The AAVSO light curve shows that V1223 Sgr is usually found within  $\pm 0.5$  mag of  $V = 13.0$ . Unfortunately, we do not have simultaneous AAVSO data at the epoch of the *Spitzer* observations. However, accretion disk events are most dramatic in the optical and UV for CVs, and it strains credulity that an event of this type could create a 2.8 mag change in the mid-infrared (note the changing SED for SS Cyg, discussed below).

Given that the spectral slope of the LL2 data for V1223 Sgr and AE Aqr are identical,  $F_\nu \propto \nu^{-0.7}$ , suggests that the best explanation for the flaring event from V1223 Sgr is optically thin synchrotron emission. But before we make this leap, we investigate whether this flare could be consistent with free-free emission, perhaps from some type of transient accretion disk wind. The *Hubble Space Telescope* parallax (Beuermann et al. 2004) shows that V1223 Sgr is at a distance of 500 pc. At this distance, assuming an isotropic source, the differential LL2 luminosity at the peak was  $L = 1.2 \times 10^{32}$  erg  $\text{s}^{-1}$ .

We estimate that the semimajor axis of the V1223 Sgr system is 0.006 AU. If we assume that the accretion disk extends to 60% of this radius, and we use a cylindrical volume with a height equal  $0.1 R_{\text{disk}}$ , we get a volume of  $V \sim 8 \times 10^{31}$   $\text{cm}^3$ . Following the example of K rding et al. (2008), we will assume that  $10^{-8} M_\odot$ , approximately one year of mass accretion for this system, is involved in this wind. This leads to a density of  $n_e = 2.6 \times 10^{-7}$   $\text{cm}^{-3}$ . The total luminosity of this emitting volume is  $L_{\text{ff}} \approx 8.7 \times 10^{-7}$  erg  $\text{s}^{-1}$ . As discussed by K rding et al., to even get close to explaining the observed flux by free-free emission will require collimation of the wind into very small opening angles, while carrying the entire accreted mass. Such a model is highly unrealistic.

The solution, of course, is evident by comparing the behavior of V1223 Sgr to AE Aqr, an IP that has been shown to be a synchrotron source. For example, Dubus et al. (2004) show that AE Aqr is highly variable in the mid-infrared at a level similar to what we have found for V1223 Sgr. They found that at 17.5  $\mu\text{m}$  (corresponding to the mean wavelength of the LL2 spectra),

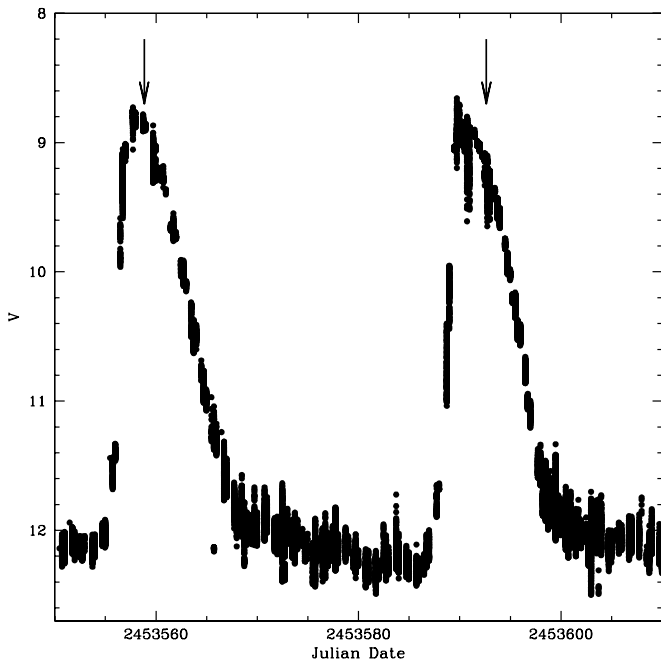


**Figure 7.** AAVSO light curve of SS Cyg during the time of the two *Spitzer* observations (arrowed).

AE Aqr has an average flux of 26.8 mJy, though the peak flux exceeded 40 mJy. We found that the mean flux for AE Aqr from the LL2 data presented in Paper I was 33 mJy. These values are similar to the peak flux observed for V1223 Sgr. The difference, of course, is that V1223 Sgr is five times more distant than AE Aqr, and thus is much more luminous. Unfortunately, we do not have sufficient wavelength coverage (compared to Dubus et al. 2007) to more fully explore their similarities. We conclude that the best model to explain the *Spitzer* observations of V1223 Sgr are that they are due to the detection of optically thin synchrotron emission, presumably in a collimated outflow.

#### 4.1. *Spitzer* and IRAS Observations of SS Cygni

With the radio detection of SS Cyg, and the proven capabilities of the IRS in detecting optically thin synchrotron emission, it is worthwhile to examine the mid-infrared data set for this system. Fortunately, SS Cyg was observed with the IRS (PI: Froning) on two separate occasions very close to the visual maxima of two successive outbursts (see Figure 7). We have extracted the IRS low-resolution SL2 ( $5.2 \mu\text{m} \leq \lambda \leq 7.7 \mu\text{m}$ ) and LL1 data sets for both epochs and present those spectra in Figure 8. We also have extracted the higher resolution “SH” spectrum ( $9.9 \mu\text{m} \leq \lambda \leq 19.8 \mu\text{m}$ ) for the first epoch. As shown in the figure, the SL2 spectrum for JD2453559 has a much lower flux, and is inconsistent with the other IRS data sets. There appeared to be a tracking issue for this particular observation, as the resulting spectrum was dramatically broader than it should have been, and even with enlarging the extraction width in the SPICE program, we could not extract a spectrum with the correct flux. Both LL1 data sets appear to have identical fluxes and spectral shapes, and the SH data set for JD2453559 appears to smoothly transition between the SL2 data set for JD2453592, and both of the LL1 spectra. Thus, the mid-IR spectra for both epochs were very similar.

As shown in this figure, the outburst photometry (from Szkody 1977) for SS Cyg can be fitted by a single temperature (10,500 K) blackbody (with  $A_V = 0.12$ ), from the *U* band

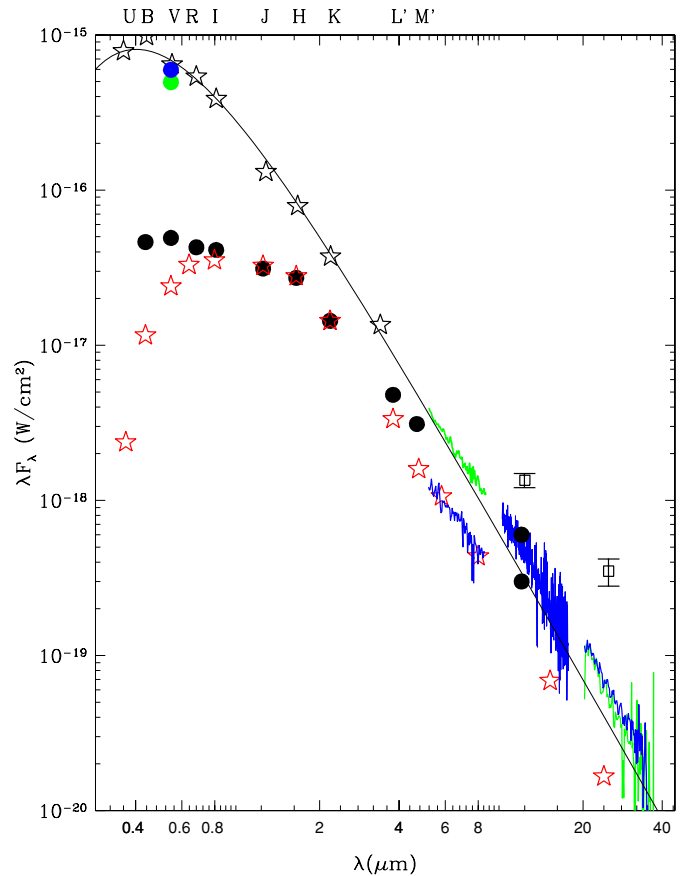


**Figure 8.** *Spitzer* IRS spectra of SS Cyg for JD2453559 (blue) and JD2453592 (green). As noted in the text, there was an apparent tracking issue during the SL2 spectrum for JD2453559, and its flux is much lower than expected. The blue and green filled circles correspond to the *V*-band magnitudes at the time of the *Spitzer* observations. The black star symbols are outburst *UBVRIJHKL* photometry from Szkody (1977). These data have been fit by a reddened ( $A_V = 0.12$  mag) blackbody with  $T_{\text{eff}} = 10,500$  K. The black filled circles are the quiescent photometry from Dubus et al. (2004), including the “flare” they observed at  $11.6 \mu\text{m}$ . The red stars are the expected fluxes from a K5 dwarf normalized to the *K*-band magnitude, with mid-infrared fluxes estimated using the *Spitzer* STAR-PET (<http://ssc.spitzer.caltech.edu/tools/starpet/>) tool. The open squares with error bars are the *IRAS* measurements from Jameson et al. (1987).

through the *L* band. The quiescent photometry (from Dubus et al. 2004) is shown as filled black circles. As discussed in Harrison et al. (2007), the quiescent SED is dominated by the K5 secondary star from *I* through *K*, but shows a weak excess beyond  $3 \mu\text{m}$ . They modeled this excess with an optically thin bremsstrahlung component. Note that Dubus et al. also observed highly variable  $11.7 \mu\text{m}$  emission from SS Cyg, the peak flux of which is also plotted in Figure 8. If one adds the quiescent K star SED to the 10,500 K blackbody model, the IRS data can be explained, and there is no evidence for an excess in the mid-IR spectra. Obviously, the fit of such a model depends on how well this hot blackbody represents the outburst fluxes in the mid-infrared, and its actual normalization at the time of the *Spitzer* observations.

Also plotted in Figure 8 is the average of the *IRAS* detections of SS Cyg from Jameson et al. (1987). As demonstrated in their Figure 1, the *IRAS* detections of SS Cyg took place earlier in the outburst than the *Spitzer* observations presented above, and more closely correspond to the period in the outburst where the peak radio flux was observed by Körding et al. (2008). Jameson et al. invoked a dust shell model to explain the *IRAS* detections, as

they could not achieve the observed fluxes with bremsstrahlung emission in any plausible scenario. Obviously, the lack of the detection of this dust in the new *Spitzer* observations rules out a static shell. We believe the *IRAS* observations are the detection of the optically thin synchrotron emission from the radio jet. If the mid-IR flux exactly followed the outburst radio light curve, one would estimate that the 25  $\mu\text{m}$  flux of the synchrotron source would be  $\sim 25\%$  of the peak outburst flux at the point in the light curve corresponding to the time of the *Spitzer* observations. Given that the mean *IRAS* band II flux was 29.2 mJy, implies a flux density of  $\sim 7$  mJy at 25  $\mu\text{m}$  for the *Spitzer* observations of SS Cyg, which is consistent with both LL1 spectra.

## 5. CONCLUSIONS

The large mid-infrared flare observed from V1223 Sgr can only be reconciled with synchrotron emission. To keep the luminosity of the event from being very large, would argue for a collimated source. Thus, along with AE Aqr and SS Cyg, we now add another CV to the list of synchrotron sources. It is obvious that the synchrotron emission from CVs is highly variable. It would be worthwhile to obtain additional mid-infrared and radio observations of V1223 Sgr to establish the duty cycle of this emission, as well as coordinated X-ray observations to establish if the spin or orbital period have any role in the timing of the emission from V1223 Sgr. Fortunately, both the *WISE* and *Herschel* missions will allow further investigation of CVs in the mid-infrared to survey how common synchrotron emission is, as well as expanding the search to cover all subclasses of CVs.

This work is based in part on observations made with the *Spitzer Space Telescope*, which is operated by the Jet Propulsion Laboratory, California Institute of Technology under a contract

with NASA. Support for this work was provided by NASA through an award issued by JPL/Caltech. We acknowledge with thanks the variable star observations from the AAVSO International Database contributed by observers worldwide and used in this research.

## REFERENCES

- Belle, K. E., Howell, S. B., Mukai, K., Szkody, P., Nishikida, K., Ciardi, D. R., Fried, R. E., & Oliver, J. P. 2005, *AJ*, **129**, 1985
- Beuermann, K., Harrison, T. E., McArthur, B. E., Benedict, G. F., & Gänsicke, B. T. 2004, *A&A*, **419**, 291
- Dubus, G., Campbell, R., Kern, B., Taam, R. E., & Spruit, H. C. 2004, *MNRAS*, **349**, 869
- Dubus, G., Tamm, R. E., Hull, C., Watson, D. M., & Mauerhan, J. C. 2007, *ApJ*, **663**, 516
- Gallo, E., Migliari, S., Markoff, S., Tomsick, J., Bailyn, C., Berta, S., Fender, R., & Miller-Jones, J. 2007, *ApJ*, **670**, 600
- Gelino, D. M., Gelino, C. R., & Harrison, T. E. 2010, *ApJ*, submitted
- Harrison, T. E., Campbell, R. K., Howell, S. B., Cordova, F. A., & Schwope, A. D. 2007, *ApJ*, **656**, 444
- Harrison, T. E., Johnson, J. J., McArthur, B. E., Benedict, G. F., Szkody, P., Howell, S. B., & Gelino, D. M. 2004, *AJ*, **127**, 460
- Hellier, C., Mukai, K., Ishida, M., & Fujimoto, R. 1996, *MNRAS*, **280**, 877
- Houck, J. R., et al. 2004, *ApJS*, **154**, 18
- Jameson, R. F., King, A. R., Bode, M. F., & Evans, A. 1987, *Observatory*, **107**, 72
- Körding, E., Rupen, M., Knigge, C., Fender, R., Dhawan, V., Templeton, M., & Muxlow, T. 2008, *Science*, **320**, 1318
- Livio, M. 1999, *Phys. Rep.*, **311**, 225
- Migliari, S., & Fender, R. 2006, *MNRAS*, **366**, 79
- Norton, A. J., Wynn, G. A., & Somerscales, R. V. 2004, *ApJ*, **614**, 349
- Ramsay, G., Wheatley, P. J., Norton, A. J., Hakala, P., & Baskill, D. 2008, *MNRAS*, **387**, 1157
- Ritter, H., & Kolb, U. 2003, *A&A*, **404**, 301
- Soker, N., & Lasota, J.-P. 2004, *A&A*, **422**, 1039
- Szkody, P. 1977, *ApJ*, **217**, 140
- van Amerongen, S., & van Paradijs, J. 1989, *A&A*, **219**, 195
- Wickramasinghe, D. T., Wu, K., & Ferrario, L. 1991, *MNRAS*, **249**, 460